

AD-A164 159

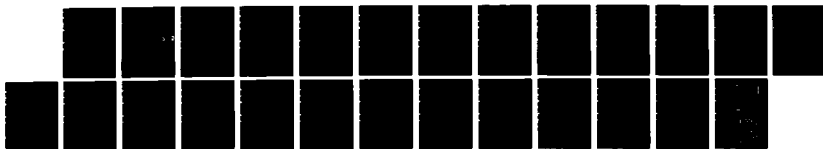
A QUANTUM MECHANICAL INVESTIGATION OF VIBRATIONAL
ENERGY TRANSFER IN O (((U) AEROSPACE CORP LOS ANGELES
CA CHEMISTRY AND PHYSICS LAB B R JOHNSON 15 JAN 86
TR-0086(6945-84)-2 SD-TR-85-85

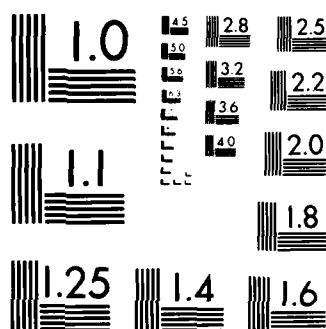
1/1

UNCLASSIFIED

F/G 7/4

ML





MICROCOPY RESOLUTION TEST CHART
NBS 1963-A

12

AD-A164 159

A Quantum Mechanical Investigation
of Vibrational Energy Transfer in
 $O(^3P) + H_2O$ Collisions

B. R. JOHNSON
Chemistry and Physics Laboratory
Laboratory Operations
The Aerospace Corporation
El Segundo, CA 90245

DTIC
SELECTED
FEB 13 1986
S D

15 January 1986

APPROVED FOR PUBLIC RELEASE;
DISTRIBUTION UNLIMITED

FILE COPY


Prepared for
SPACE DIVISION
AIR FORCE SYSTEMS COMMAND
Los Angeles Air Force Station
P.O. Box 92960, Worldway Postal Center
Los Angeles, CA 90009-2960

This report was submitted by The Aerospace Corporation, El Segundo, CA 90245, under Contract No. F04701-85-C-0086 with the Space Division, P.O. Box 92960, Worldway Postal Center, Los Angeles, CA 90009-2960. It was reviewed and approved for The Aerospace Corporation by S. Feuerstein, Director, Chemistry and Physics Laboratory.

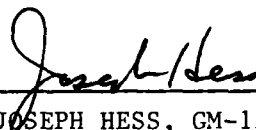
Lt LeRoy Pedone, SD/YNCS, was the project officer for the Mission-Oriented Investigation and Experimentation (MOIE) Program.

This report has been reviewed by the Public Affairs Office (PAS) and is releasable to the National Technical Information Service (NTIS). At NTIS, it will be available to the general public, including foreign nationals.

This technical report has been reviewed and is approved for publication. Publication of this report does not constitute Air Force approval of the report's findings or conclusions. It is published only for the exchange and stimulation of ideas.



LE ROY PEDONE, Lt, USAF
MOIE Project Officer
SD/YNCS



JOSEPH HESS, GM-15
Director, AFSTC West Coast Office
AFSTC/WCO OL-AB

UNCLASSIFIED

SECURITY CLASSIFICATION OF THIS PAGE (When Data Entered)

REPORT DOCUMENTATION PAGE		READ INSTRUCTIONS BEFORE COMPLETING FORM
1. REPORT NUMBER SD-TR-85-85	2. GOVT ACCESSION NO.	3. RECIPIENT'S CATALOG NUMBER
4. TITLE (and Subtitle) A. QUANTUM MECHANICAL INVESTIGATION OF VIBRATIONAL ENERGY TRANSFER IN O (³ P) + H ₂ O COLLISIONS		5. TYPE OF REPORT & PERIOD COVERED
		6. PERFORMING ORG. REPORT NUMBER TR-0086(6945-04)-2
7. AUTHOR(s) Bernard R. Johnson		8. CONTRACT OR GRANT NUMBER(s) F04701-85-C-0086
9. PERFORMING ORGANIZATION NAME AND ADDRESS The Aerospace Corporation El Segundo, Calif. 90245		10. PROGRAM ELEMENT, PROJECT, TASK AREA & WORK UNIT NUMBERS
11. CONTROLLING OFFICE NAME AND ADDRESS Space Division Los Angeles Air Force Station Los Angeles, Calif. 90009-2960		12. REPORT DATE 15 January 1986
		13. NUMBER OF PAGES 21
14. MONITORING AGENCY NAME & ADDRESS (if different from Controlling Office)		15. SECURITY CLASS. (of this report) Unclassified
		15a. DECLASSIFICATION/DOWNGRADING SCHEDULE
16. DISTRIBUTION STATEMENT (of this Report) Approved for public release; distribution unlimited		
17. DISTRIBUTION STATEMENT (of the abstract entered in Block 20, if different from Report)		
18. SUPPLEMENTARY NOTES		
19. KEY WORDS (Continue on reverse side if necessary and identify by block number) Inelastic Collisions Infinite Order Sudden Approximation Vibrational Excitation		
20. ABSTRACT (Continue on reverse side if necessary and identify by block number) Cross sections for the vibrational excitation of H ₂ O in collision with O(³ P) are calculated for relative collision energies of 0.5 to 3.0 eV by the vibrational close-coupling rotational infinite order sudden method using an accurate potential energy surface. The excitation cross sections obtained by this quantum mechanical calculation are compared to results of a recently published quasiclassical trajectory study which used the same potential surface. Very large differences between the quantum mechanical and classical trajectory results are found.		

CONTENTS

I.	INTRODUCTION.....	7
II.	CALCULATIONS.....	11
	A. Potential Energy Function.....	11
	B. Dynamics.....	11
	C. Numerical Techniques.....	14
	D. Convergence Tests.....	14
III.	RESULTS AND DISCUSSION.....	21
IV.	CONCLUSIONS.....	23
	REFERENCES.....	25

Accession For	
NTIS CRA&I	<input checked="" type="checkbox"/>
DTIC TAB	<input type="checkbox"/>
Unannounced	<input type="checkbox"/>
Justification	
By	
Distribution/	
Availability Codes	
Dist	Avail and/or Special
A-1	

FIGURES

1. Plot Showing the Convergence of the 010 Cross Sections
With Respect to the Expansion Basis Set..... 17
2. Plot Showing the Convergence of the 001 Cross Sections
With Respect to the Expansion Basis Set..... 18
3. Cross Sections for the Collisional Excitation of Ground
State H_2O by $\text{O} (^3\text{P})$ to the Single Quanta Vibrational
States 010, 100, and 001..... 22

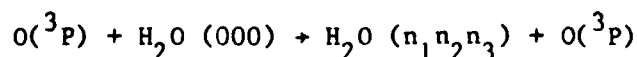
TABLE

1. H ₂ O Vibrational Energy Levels in eV.....	16
----------------------------------------------------------	----

I. INTRODUCTION

In recent years an effort has been made to determine the collision cross sections for the vibrational excitation of H_2O by $\text{O}(^3\text{P})$. This work has consisted of both experimental measurements and theoretical calculations. The measurements, which were carried out by Dunn and co-workers in a rather difficult shock tube experiment, could provide only a limited amount of data.¹ In order to extend these data, a theoretical program was initiated by Redmon and Bartlett.²⁻⁴ They calculated an accurate $\text{O}-\text{H}_2\text{O}$ potential energy surface and then used this surface to calculate the inelastic cross sections by the quasiclassical trajectory method. The results they obtained were in fair agreement with the limited experimental data available. This is encouraging; however, it is not definitive since both the theory and experiment are subject to a great deal of uncertainty. Other theoretical calculations and experimental measurements would be very useful in judging their ultimate accuracy. For this reason we have decided that an approximate quantum mechanical calculation of the $\text{O} + \text{H}_2\text{O}$ collision problem, employing the same potential surface as the classical trajectory calculation, would be a useful test. In addition, from a purely theoretical point of view, we are comparing two widely used techniques and testing them (against each other) in new physical regimes.

In this report, we present the results of a quantum mechanical calculation of the vibrational excitation cross sections for the reaction



where n_1 , n_2 , and n_3 are the symmetric stretch, bend, and asymmetric stretch vibrational quantum numbers, respectively. The relative collision energies considered in this study range from 0.5 to 3.0 eV, and the final vibrational states are (010), (100), and (001). We use the vibrational close-coupling-infinite order sudden (VCC-IOS) method to treat the collision dynamics and use the same potential surface as Redmon and Bartlett in their classical trajectory calculation. Thus, our study will give a direct comparison of

the VCC-IOS and classical trajectory methods for this important problem.

The application of the VCC-IOS method to atomic scattering from both linear⁵ and nonlinear⁶ triatomic targets has been pioneered in recent years by D.C. Clary. The method, which was originally developed to study atom diatomic molecule scattering, incorporates an exact close-coupling treatment of the vibrational degrees of freedom along with an IOS approximation treatment of the rotational degrees of freedom. This method is justified, theoretically, when the rotational energy spacings are very small in relation to the translational and vibrational energies, and has been applied with great success in such cases. When the molecule is a hydride, as in the present case, the rotational spacings are much larger, so the method has less justification. This pessimistic evaluation would certainly apply if we were attempting to calculate transitions to a specific vibration-rotation state. However, in the present problem, we are calculating vibrational transitions without regard to the final rotation state, i.e., we sum over the final rotations. Empirical evidence cited subsequently indicates that these summed cross sections can indeed be calculated accurately, even for hydride molecules.

Our justification for applying the VCC-IOS method to the O-H₂O problem is based on the success this method has had in describing atom-diatomic molecule and also atom-symmetric top inelastic scattering problems. In particular we refer to the two rather severe tests of the VCC-IOS method given in references 7 and 8, where the collision energies were low and the rotational energy level spacings of the target molecules--H₂ in reference 7 and NH₃ and H₂CO in reference 8--are rather widely spaced as they are for the H₂O molecule. In reference 8 it was found that all the IOS cross sections to individual rotational states were in qualitative accord with accurate values, and for most the agreement was within 20%. The most important result obtained in reference 7 is the observation that the IOS cross sections, summed over final states, are accurate, even for very low collision energies. If we sum the cross sections given in reference 8 over final states, we can verify that in this case also, the summed IOS cross sections are quite accurate.

Another justification for using the VCC-IOS approximation in the present problem is based on the good agreement between exact classical trajectory and classical sudden approximation calculations of vibrationally inelastic cross sections for the $\text{O-H}_2\text{O}$ collision. Redmon et al.² report that the classical exact and classical sudden approximation results agree within a factor of 2 for this problem.

II. CALCULATIONS

A. POTENTIAL ENERGY FUNCTION

The O-H₂O potential energy surface (PES) used in this investigation is the same PES employed by Redmon and Bartlett et al.^{2,3} to carry out their classical trajectory study. This surface is an analytic fit to ab-initio generated points, which they calculated by means of many body perturbation theory. They made several fits to the PES. The particular fit used in this study is the surface that they have designated as E_{3a}. A complete discussion of this surface, the ab-initio calculations, and the fitting procedure is contained in the reports by Redmon et al.²⁻⁴ and references therein.

B. DYNAMICS

Since the application of the VCC-IOS method to atom-nonlinear (X-ABC) triatomic molecule collisions is described in detail elsewhere,⁶ we will mention here only a few salient facts in order to fix the notation of the present report. An appropriate set of coordinates to describe this problem are the three Eulerian angles α , β , and γ , which determine the orientation of the Eckart coordinate frame for the triatomic molecule; the three normal mode vibration coordinates Q_1 , Q_2 , and Q_3 , which determine the position vectors of the three molecular atoms (A,B,C) in the Eckart frame;⁹ and finally the three spherical coordinates R , θ , and ϕ of the colliding atom (X) relative to the Eckart frame. The molecule lies in the xy plane with its center of mass at the origin of the Eckart frame. The Schroedinger equation in this coordinate system is

$$\left(-\frac{\hbar^2}{2\mu R} \frac{\partial^2}{\partial R^2} R + \frac{L^2}{2\mu R^2} + H_{ABC} + V_{int} - E \right) \psi = 0 \quad (1)$$

where μ is the reduced mass, L is the angular momentum operator for the incident atom, H_{ABC} is the Hamiltonian for the isolated triatomic molecule, E is the total energy, and V_{int} (which is a function of Q_1 , Q_2 , Q_3 , R , θ , and ϕ) is the interaction potential.

In the VCC-IOS approximation, the vibration-rotation Hamiltonian H_{ABC} is replaced by the simpler zero angular momentum vibrational Hamiltonian¹⁰ H_{ABC}^v , and the angular momentum operator is replaced by the eigenvalue form $\hbar^2 \ell(\ell + 1)$. The result is an extreme simplification. All the angular variables $\alpha, \beta, \gamma, \theta$, and ϕ are decoupled from the dynamics, although θ and ϕ remain in the wavefunction as parameters. The resultant Schroedinger equation is then solved by the usual close-coupling technique in which the wavefunction is expanded in the following basis function representation

$$\psi = \sum_n f_n^{\ell} (R|\theta, \phi) \Gamma_n(Q_1, Q_2, Q_3)/R \quad (2)$$

The basis functions, $\Gamma_n(Q_1, Q_2, Q_3)$, are the zero angular momentum vibration states of the isolated triatomic molecule, i.e., they are the eigenfunction solutions of the equation

$$(H_{ABC}^v - E_n) \Gamma_n(Q_1, Q_2, Q_3) = 0. \quad (3)$$

The index n in the above expressions represents the collection of three normal mode vibrational quantum numbers $(n_1 n_2 n_3)$. Equation (3) is solved by the method described by Whithead and Handy¹¹ in which the basis functions $\Gamma_n(Q_1, Q_2, Q_3)$ are expanded in a "primitive basis set"

$$\begin{aligned} \Gamma_n(Q_1, Q_2, Q_3) = & \sum_{j_1=0}^{N_1} \sum_{j_2=0}^{N_2} \sum_{j_3=0}^{N_3} a(n|j_1, j_2, j_3) Q_1^{j_1} Q_2^{j_2} Q_3^{j_3} \\ & \times \exp [-(\omega_1 Q_1^2 + \omega_2 Q_2^2 + \omega_3 Q_3^2)/2] \end{aligned} \quad (4)$$

Here the N_i are integers, and ω_i are the fundamental normal mode vibration frequencies of the triatomic molecule.

Equation 2 is substituted into the VCC-IOS simplified version of Eq. (1), multiplied by $\Gamma_n(Q_1, Q_2, Q_3)$, and integrated over the $\{Q_i\}$ to obtain the vibrational close-coupled differential equations

$$\left[\frac{d^2}{dR^2} + k_n^2 - \frac{\ell(\ell+1)}{R^2} \right] f_n^\ell(R; \theta, \phi) = \frac{2\pi}{\hbar^2} \sum_{n'=1}^N V_{n,n'}(R; \theta, \phi) f_{n'}^\ell(R; \theta, \phi) \quad (5)$$

where

$$k_n^2 = \frac{2\mu}{\hbar^2} (E - E_n) \quad (6)$$

and

$$V_{n,n'}(R; \theta, \phi) = \int_{-\infty}^{\infty} \int_{-\infty}^{\infty} \int_{-\infty}^{\infty} dQ_1 dQ_2 dQ_3 \Gamma_n(Q_1, Q_2, Q_3) V_{int}(Q_1, Q_2, Q_3, R, \theta, \phi) \Gamma_{n'}(Q_1, Q_2, Q_3) \quad (7)$$

The decoupled variables ℓ , θ , and ϕ appear as parameters in Eq. (5). For each assigned set of parameter values, the coupled equations are integrated, subject to standard scattering boundary conditions, to calculate the S matrix elements, $S_{n,n'}^\ell(\theta, \phi)$. Finally, the vibrational excitation cross section, averaged over initial rotation states and summed over the final rotation states, is given by the rather simple expression⁶

$$\sigma(n \rightarrow n') = \frac{1}{k_n^2} \int_0^1 \int_{-\pi/2}^{\pi/2} dx d\phi \sum_{\ell} (2\ell+1) |\delta_{n,n'} - S_{n,n'}^\ell(x, \phi)|^2 \quad (8)$$

where $x = \cos \theta$. We have made use of the symmetry of H_2O molecule to reduce the integration range of both the x and ϕ variables.

C. NUMERICAL TECHNIQUES

The computer code used to carry out the calculations is basically the same as that used by Clary⁶ in his $He + SO_2$ calculations except for the modifications described subsequently.

We determined that it was not necessary to integrate the scattering equations for every ℓ value in the range $0 \leq \ell \leq \ell_{\max}$. Instead, the code was modified to calculate for every tenth ℓ value and to interpolate the intervening values. This resulted in a substantial savings in computation time.

The numerical quadrature in Eq. (8) was changed from a two-dimensional Simpson rule to a Monte Carlo procedure. Using this method, one can easily add additional integration points, if needed, without discarding previously calculated points. This consideration, combined with our modest accuracy requirement that the integral be converged to about 20% made the low order Monte Carlo procedure a practical alternative to the higher order Simpson rule. Using this method, Eq. (8) becomes

$$\sigma(n \rightarrow n') = \frac{1}{Mk_n^2} \sum_{i=1}^M \sum_{\ell} (2\ell+1) |\delta_{nn'} - S_{nn'}^{\ell}(x_i, \phi_i)|^2 \quad (9)$$

where the M values of x_i and ϕ_i are selected at random with uniform distribution in the ranges $0 \leq x_i \leq 1$ and $-\pi/2 \leq \phi_i \leq \pi/2$. We selected $M = 25$, which gives a nominal convergence of 20%.

D. CONVERGENCE TESTS

A number of input parameters to the computer code, which control the accuracy of the calculation, must be determined, primarily by trial and error. As a rule, any change in parameter values that increases the accuracy of the computed cross sections also increases the time and therefore the cost of the calculation. In general, we adjusted the following parameters to obtain about 5% convergence: The lower and upper integration limits on the

radial variable R in Eq. (5) were set at 2 and 11 bohr, respectively. The actual method for obtaining the scattering solution to this equation was by R -matrix propagation. To carry out this calculation, the integration range was divided into 100 equally spaced propagation sectors. The maximum angular momentum quantum number was set to $l_{\text{max}} = 200$. This value was determined to be sufficient at the highest relative translational kinetic energy, 3.0 eV, and was used in most of the calculations.

A number of trial calculations were performed to test for convergence with respect to the basis set expansion. In these tests, we varied the number of primitive basis functions by varying the parameters N_1 , N_2 , and N_3 [see Eq. (4)] and also by varying N , the number of channels in the close-coupled equations [see Eq. (5)]. We have determined that the minimum basis set required to obtain reasonably well converged cross sections is given by $N_1 = N_3 = 2$, $N_2 = 3$, and $N = 10$. It is of some interest to compare the energy levels of the 10 basis functions, calculated using this primitive basis set, to the accurate values of the vibrational energy levels for H_2O . This comparison is given in Table 1, where the states are labeled by the standard vibrational quantum number designation. Although the calculated levels are not accurate by spectroscopic standards, they are "good enough," as shown by our convergence tests, to serve as a basis set for the scattering calculations. The vibrational quantum numbers n_1 , n_2 , and n_3 have a simple interpretation¹²--they count the number of nodes in the wavefunction; n_1 counts nodes along the Q_1 coordinate, n_2 counts nodes along Q_2 , and n_3 counts nodes along Q_3 . The primitive basis set we are using has a maximum of three bend nodes. This is the reason the 0,4,0 state is missing from our computed basis functions.

In order to adequately test the convergence of the scattering calculations, it is not sufficient to simply increase the number of channels, N , but we must also ensure that in doing so we have increased the number of nodes in the basis set for each of the three vibrational modes that is being tested. In Figs. 1 and 2 we show the changes that occur in the cross sections for the excitation of the 010 and 001 (i.e., the bend and asymmetric stretch)

Table 1. H₂O Vibrational Energy Levels in eV

$(n_1 \ n_2 \ n_3)$	Calculated ^a	Accurate ^b
0 0 0	0. 0	0. 0
0 1 0	0.202	0.198
0 2 0	0.401	0.391
1 0 0	0.464	0.453
0 0 1	0.478	0.466
0 3 0	0.614	0.579
1 1 0	0.664	0.648
0 1 1	0.677	0.661
0 4 0	-	0.762
1 2 0	0.857	0.838
0 2 1	0.874	0.851

^aThese levels are the eigenvalues obtained by solving Eq. (3) using the primitive basis, Eq. (4), with $N_1 = 2$, $N_3 = 2$, and $N_2 = 3$. The corresponding eigenfunctions form the basis set used in the close-coupling scattering calculations.

^bEnergy levels of sufficient accuracy were calculated using Eq. (II,268) and Eq.(III,57) in reference 13.

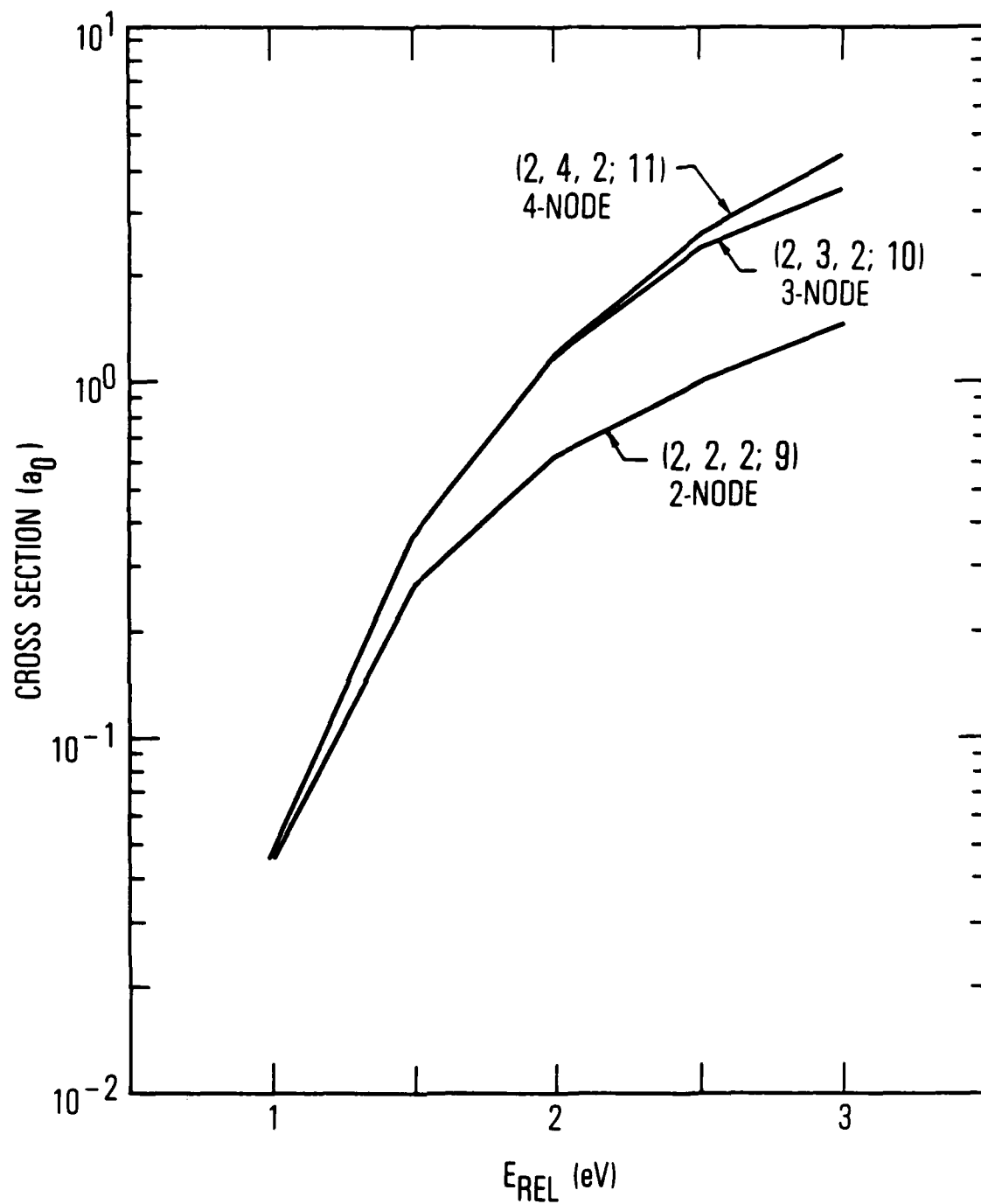


Fig. 1. Plot Showing the Convergence of the 010 Cross Sections with Respect to the Expansion Basis Set. The labels are explained in the text.

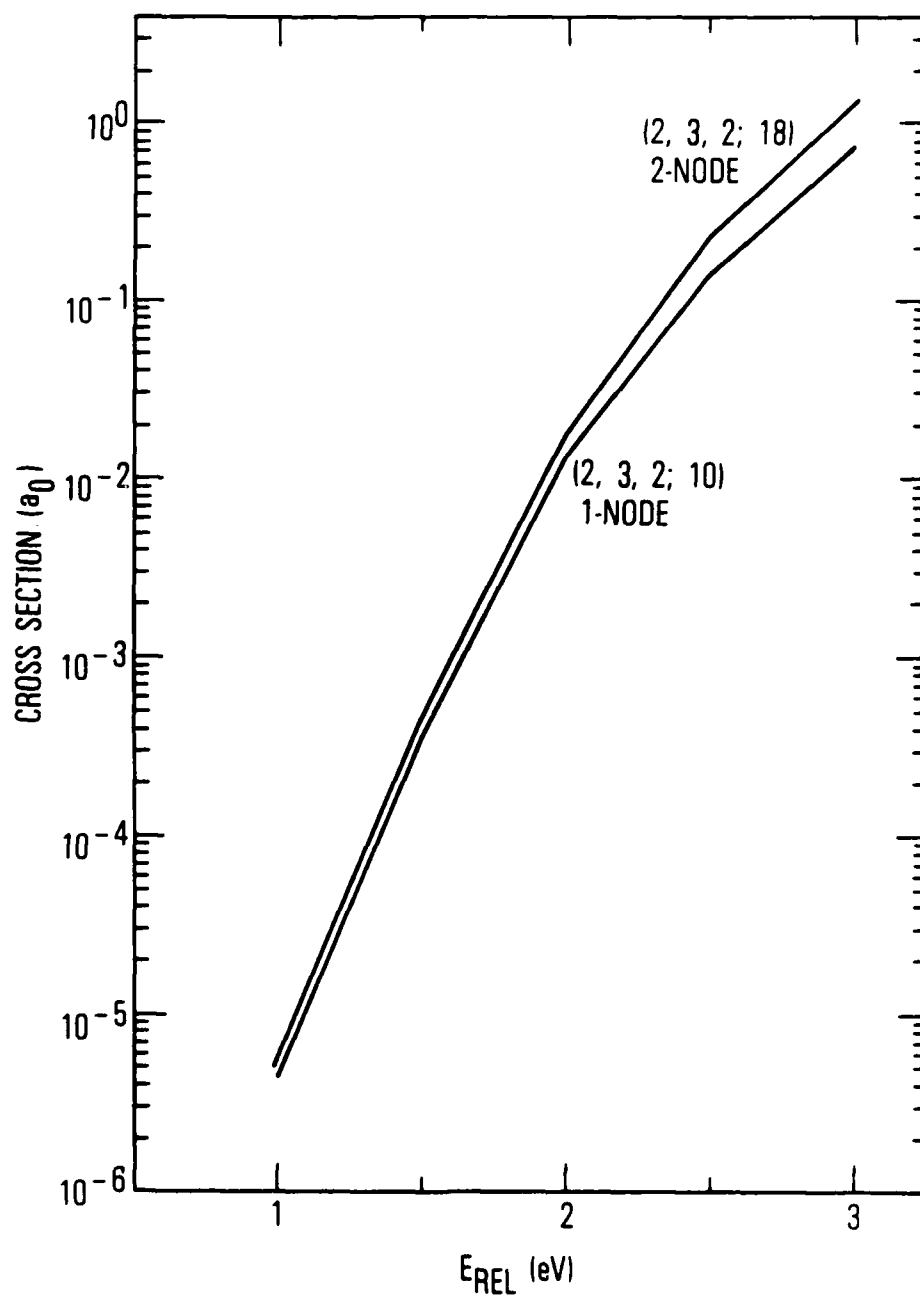


Fig. 2. Plot Showing the Convergence of the 001 Cross Sections with Respect to the Expansion Basis Set. The labels are explained in the text.

states when the basis set is enlarged to include an extra node in the respective vibrational states. In these figures, the cross section curves are labeled by $(N_1, N_2, N_3; N)$, which completely describes the basis set used in its calculation. We have also indicated the maximum number of nodes in the expansion basis sets. In Fig. 1 this refers to the bend nodes along Q_2 , and in Fig. 2 it refers to the asymmetric stretch nodes along Q_3 . The cross sections shown in Figs. 1 and 2 were calculated for a single value of the relative orientation angles θ and ϕ . (The values used were $\theta = 90$ deg and $\phi = -7$ deg.) We have not shown the convergence test of the symmetric stretch 100; it is very similar to the asymmetric 001 case.

In addition to showing the change due to increasing the number of nodes along Q_2 in Fig. 1, we also show the large change in cross section for excitation of the bend state when we reduce the number of bend nodes from three to two. This clearly shows that at least three bend nodes are required for reasonable convergence of the 010 bend excitation cross section.

Many additional tests were also carried out in which we altered the primitive basis so that we could add even more symmetric and asymmetric stretch nodes (at the expense of fewer bend nodes). The results obtained indicate that the symmetric and asymmetric stretch excitation cross sections to the states 100 and 001 are essentially insensitive to the addition of these extra nodes to the basis. This test is somewhat artificial, since we had to reduce the bend states in the basis set to less than optimum; however, we believe it is still a valid test of convergence of the stretch excitation cross sections with respect to the addition of extra stretch nodes to the basis set.

Our conclusion is that we believe our cross section calculations are adequately converged with respect to the expansion basis set and that the degree of this convergence can be judged approximately by a comparison of the curves plotted in Figs. 1 and 2. Using these criteria, the convergence for the bend excitation varies approximately from about 2 to 20%, and the convergence of the symmetric and asymmetric stretch varies from about 10 to 80%, as the relative translational energy varies from 1.0 to 3.0 eV.

Tests were also carried out to verify convergence of the Monte Carlo integration in Eq. (9). The number of integration points were increased to $M = 50$ and $M = 100$ for each of the two collision energies $E = 2$ and $E = 3$ eV. These tests verify our estimate that the calculations carried out using $M = 25$ have converged to a nominal 20% relative accuracy.

III. RESULTS AND DISCUSSION

The cross sections for transitions from the ground state to each of the three vibrational states 010, 100, and 001 of H_2O are shown in Fig. 3. Also shown for comparison are Redmon's classical trajectory results^{2,3} and two experimentally determined points.¹ Based on our discussion of the convergence with respect to basis set expansion and also the convergence of the Monte Carlo integration over the angles θ and ϕ , we estimate a relative error in our calculated results, which varies from about 20 to 40% for the 010 curve and from 30 to 100% for the 100 and 001 curves.

The low values of these error estimates apply at the low collision energies and increase to upper values at 3.0 eV. To these errors, we must also add the error resulting from the use of the rotational sudden approximation. This error is much more difficult to estimate. If we assume that the sudden approximation is correct to within a factor of 2, as has been reported for the classical calculation of this system, then the maximum combined uncertainty in our cross sections will be about a factor of 4. Even if we assumed a much larger error factor, it is obvious from Fig. 3 that a very serious disagreement exists between our VCC-IOS calculated cross sections and the classical trajectory results. Both calculations used the same potential energy surface, eliminating this as a source of any difference.

Previously, a similar comparison between classical trajectory and VCC-IOS calculated cross sections was carried out for the O-CO_2 collision.^{15,16} In that case, contrary to the present $\text{O-H}_2\text{O}$ problem, the agreement between the two methods was fairly good, i.e., within a factor of 2.¹⁶

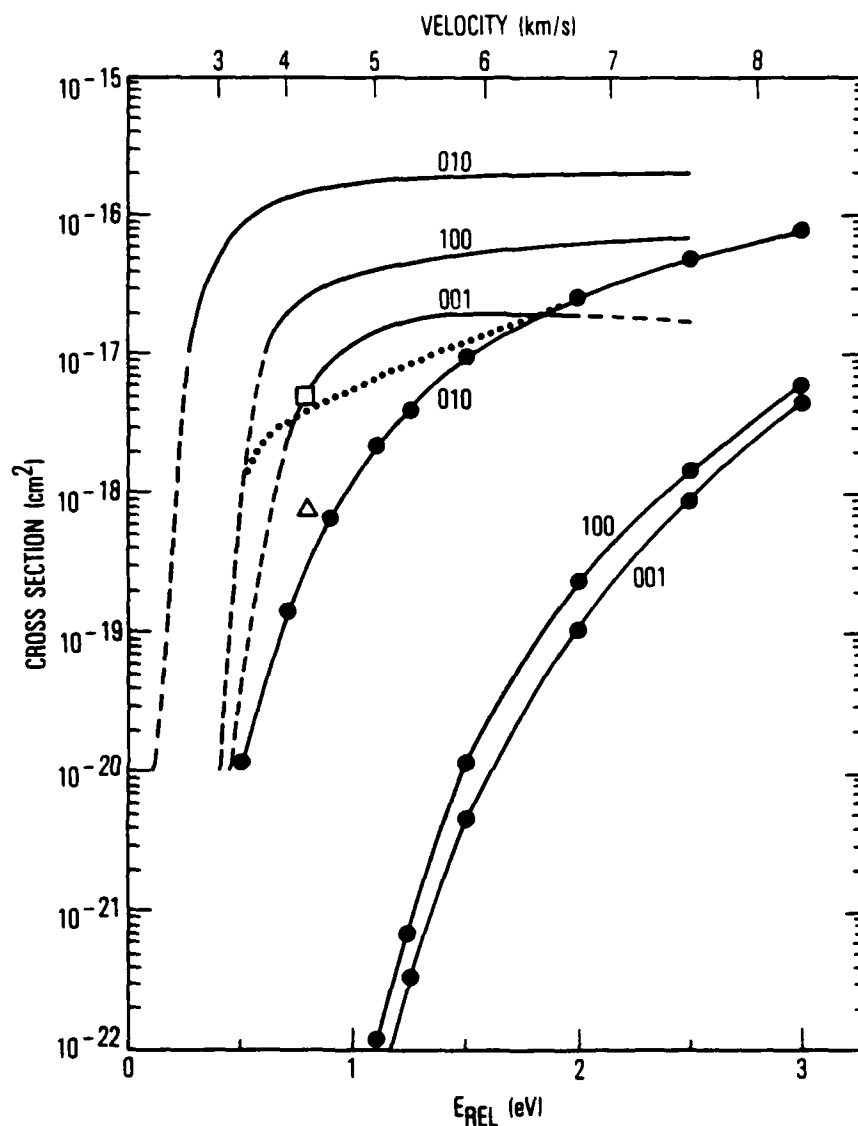


Fig. 3. Cross Sections for the Collisional Excitation of Ground State H₂O by O(³P) to the Single Quanta Vibrational States 010, 100, and 001. Lower three curves are present results, computed by VCC-IOS method. Upper three curves, taken from reference 2, were computed by classical trajectory method. Dotted curve, taken from reference 14, is a later and more accurate classical trajectory calculation of the 001 cross sections. The points Δ and ◻ are experimentally determined values of the 001 and 010 cross sections from Ref. 1.

IV. CONCLUSIONS

Quantum mechanical calculations of the $O-H_2O$ collision excitation cross sections using the VCC-IOS method have been performed in the relative energy range from 0.5 to 3.0 eV. The results, which are shown in Fig. 3, are much smaller than the classical trajectory calculated cross sections obtained using the same potential energy surface. Both of these methods represent state-of-the-art techniques for chemical dynamic calculations, and both are widely used. The present problem has attempted to push both methods to new limits of applicability. The large disagreement shows that one of the methods (or possibly both) has been pushed too far. Further work should be carried out on this or similar model systems to resolve the discrepancy.

REFERENCES

1. M. G. Dunn, G. T. Skinner, and C. E. Treanor, AIAA J. **13**, 803 (1975).
2. M. J. Redmon, R. J. Bartlett, B. C. Garrett, G. D. Purvis III, P. M. Saatzler, G. C. Schatz, and I. Shavitt, Potential Energy Surfaces and Dynamic Calculations, D. G. Truhlar, ed., Plenum, New York (1981), pp. 771-803.
3. R. J. Bartlett and M. J. Redmon, Collisional Excitation of H₂O and CO₂ by O(³P) Atoms, AFRPL-TR-81-27.
4. M. J. Redmon and G. C. Schatz, J. Chemical Phys. **54**, 365 (1981).
5. D. C. Clary, J. Chem. Phys. **75**, 209 (1981).
6. D. C. Clary, J. Chem. Phys. **75**, 2899 (1981).
7. G. Pfeffer and D. Secrest, J. Chem. Phys. **67**, 1394 (1977).
8. S. Green, J. Chem. Phys. **70**, 816 (1979).
9. E. B. Wilson, Jr., J. C. Decius, and P. C. Cross, Molecular Vibrations, McGraw-Hill, New York (1955).
10. J. K. G. Watson, Mol. Phys. **15**, 479 (1968).
11. R. J. Whithead and N. C. Handy, J. Molec. Spectroscopy **55**, 356 (1975).
12. P. Pechukas, J. Chem. Phys. **57**, 5577 (1972).
13. G. Herzberg, Molecular Spectra and Structure, Vol. II, Infrared and Raman Spectra of Polyatomic Molecules, Van Nostrand Company, New York (1945).
14. M. J. Redmon, L. T. Redmon, and B. C. Garrett, Collisional Excitation Cross Sections, AFRPL-TR-84-030.
15. N. Harvey, Chem. Phys. Lett. **88**, 553 (1982).
16. B. C. Garrett, Chem. Phys. Lett. **87**, 63 (1984).

LABORATORY OPERATIONS

The Aerospace Corporation functions as an "architect-engineer" for national security projects, specializing in advanced military space systems. Providing research support, the corporation's Laboratory Operations conducts experimental and theoretical investigations that focus on the application of scientific and technical advances to such systems. Vital to the success of these investigations is the technical staff's wide-ranging expertise and its ability to stay current with new developments. This expertise is enhanced by a research program aimed at dealing with the many problems associated with rapidly evolving space systems. Contributing their capabilities to the research effort are these individual laboratories:

Aerophysics Laboratory: Launch vehicle and reentry fluid mechanics, heat transfer and flight dynamics; chemical and electric propulsion, propellant chemistry, chemical dynamics, environmental chemistry, trace detection; spacecraft structural mechanics, contamination, thermal and structural control; high temperature thermomechanics, gas kinetics and radiation; cw and pulsed chemical and excimer laser development including chemical kinetics, spectroscopy, optical resonators, beam control, atmospheric propagation, laser effects and countermeasures.

Chemistry and Physics Laboratory: Atmospheric chemical reactions, atmospheric optics, light scattering, state-specific chemical reactions and radiative signatures of missile plumes, sensor out-of-field-of-view rejection, applied laser spectroscopy, laser chemistry, laser optoelectronics, solar cell physics, battery electrochemistry, space vacuum and radiation effects on materials, lubrication and surface phenomena, thermionic emission, photo-sensitive materials and infrared detectors, atomic frequency standards, and environmental chemistry.

Computer Science Laboratory: Program verification, program translation, performance-sensitive system design, distributed architectures for spaceborne computers, fault-tolerant computer systems, artificial intelligence, micro-electronics applications, communication protocols, and computer security.

Electronics Research Laboratory: Microelectronics, solid-state device physics, compound semiconductors, radiation hardening; electro-optics, quantum electronics, solid-state lasers, optical propagation and communications; microwave semiconductor devices, microwave/millimeter wave measurements, diagnostics and radiometry, microwave/millimeter wave thermionic devices; atomic time and frequency standards; antennas, RF systems, electromagnetic propagation phenomena, space communication systems.

Materials Sciences Laboratory: Development of new materials: metals, alloys, ceramics, polymers and their composites, and new forms of carbon; non-destructive evaluation, component failure analysis and reliability; fracture mechanics and stress corrosion; analysis and evaluation of materials at cryogenic and elevated temperatures as well as in space and enemy-induced environments.

Space Sciences Laboratory: Magnetospheric, auroral and cosmic ray physics, wave-particle interactions, magnetospheric plasma waves; atmospheric and ionospheric physics, density and composition of the upper atmosphere, remote sensing using atmospheric radiation; solar physics, infrared astronomy, infrared signature analysis; effects of solar activity, magnetic storms and nuclear explosions on the earth's atmosphere, ionosphere and magnetosphere; effects of electromagnetic and particulate radiations on space systems; space instrumentation.

END

FILMED

3

-86

DTIC